# Analyst

Accepted Manuscript






ROYAL SOCIETY OF CHEMISTRY

www.rsc.org/analyst

Cite this: DOI: 10.1039/c0xx00000x

www.rsc.org/xxxxxx

ARTICLE TYPE

# Trace vapour detection at room temperature using Raman spectroscopy

**Alison Chou,[a] Babak Radi,[b] Esa Jaatinen,[b] Saulius Juodkazis,[c] Peter M. Fredericks[b]**

***Received (in XXX, XXX) Xth XXXXXXXXX 200X, Accepted Xth XXXXXXXXX 200X***

**DOI: 10.1039/b000000x**

A miniaturized flow-through system consisting of a gold coated silicon substrate based on enhanced Raman spectroscopy has been used to study the detection of vapour from model explosive compounds. The measurements show that the detectability of the vapour molecules at room temperature depends sensitively on the interaction between the molecule and the substrate. The results highlight the capability of a flow system combined with Raman spectroscopy for detecting low vapour pressure compounds with a limit of detection of 0.2 ppb as demonstrated by the detection of bis(2-ethylhexyl) phthalate, a common polymer additive emitted from a commercial polyvinyl chloride (PVC) tubing at room temperature.

## Intriduction

Two key considerations in developing vapour sensing systems have been lowering the concentration of vapour required for a positive detection, as well as making the overall system as compact as possible to aid portability. Detection of vapours emitted from a hazardous solid or liquid is the preferable mode of operation as it does not require contacting the surface of the sample. However, the concentration of vapour depends on the vapour pressure of the compound and in still air at room temperature, most explosives have vapour concentrations in the range of parts per billion (ppb) to parts per trillion (ppt) and even lower for mixtures of explosive materials.[1] Capturing enough explosive material vapour in the air for detection and analysis is thus difficult.

Until the discovery of Raman scattering enhancement of pyridine adsorbed on roughened silver electrodes[2, 3] and silver nanoparticles[4] in the 1970s, the application of Raman spectroscopy in chemical sensors had been constrained by the limits of detection due to small fractions of the inelastic Raman scattering process, which typically has cross sections of the order of $10^{-30}$ to $10^{-25}$ $cm^2$/molecule.[5] Since then, the amplification of Raman scattering signals by metal nanostructures, which is now referred to as surface enhanced Raman spectroscopy (SERS), has been pursued with great interest because of its potential to substantially lower detection limits. The signal enhancement relies on the optical properties of the metal nanostructures with the mechanism depending on the surface roughness and the geometry of the experiment setup. Generally, the mechanism has been attributed to surface plasmon,[6] charge transfer,[7] and resonant light scattering.[8] Available data in the literature on SERS show many of the most sensitive methods use silver[9, 10] or gold nanoparticles[11-14] in their vapour or gas sensing scheme for signal enhancement with detection limits at the picomolar level possible.[15] More recently developed SERS flow-through vapour detection methods report a detection limit of 0.5 ppb and 1 ppb as demonstrated by Oo *et al*.[16] and Piorek *et al*.[17] respectively. Oo *et al*. used a flow through detection system where vapours of pyridine and 4-nitrophenol are passed through capillaries of various inner diameters ranging from 4.7 to 700 μm lined with gold nanoparticles on the inner walls of the capillaries. Piorek *et al*. demonstrated the detection of 2,4-dinitrotoluene (2,4-DNT) vapour using a microfluidic flow system filled with silver colloid in aqueous solution. Analyte vapours flow over the microfluidic channel and diffuse into the aqueous phase therein interacting with the silver colloid followed by detection with a Raman spectrophotometer. A disadvantage of both methods is that they require synthesis of nanoparticle systems with appropriate dimensions and specific optical properties in order to achieve their detection objectives.

This work describes a detection method that requires only a silicon substrate coated with a fresh sputtered gold film, without the complexity of incorporating nanoparticles into a polymer layer or a separate step of nanoparticles synthesis. Our flow system is constructed by adapting a modified approach based on our recently published static test of nitro compound vapour detection using Raman spectroscopy.[18] The modified detection system is an automated recirculating flow system that delivers vapours to the sensor surface allowing real-time detection. Vapours from sublimation of solid analytes at room temperature flow over a 5 $mm^2$ square silicon substrate coated with sputtered gold used for capturing vapour molecules and detection by a commercially available Raman spectrophotometer. The vibrations of the molecules on the substrate surface produce a spectrum that allows the method to detect and distinguish compounds at concentrations of a few parts per million at room temperature. The detected concentration of the analyte was estimated from the vapour

pressure of the analyte at room temperature.

The main objectives of this paper were to verify the feasibility of our proposed detection method and to assess the differences of dynamic versus static measurements. Surface fouling of gold substrates which could pose a limitation for SERS based sensor using gold is also discussed. Experiments were carried out using six explosive model compounds with vapour pressures ranging between $2\times10^{-4}$ to 0.1 mmHg at 25 °C. To demonstrate the trace detection capability of the flow system, a commercial sample of polyvinyl chloride (PVC) tubing containing bis(2-ethylhexyl) phthalate (DEHP, or DOP) was used as an analyte. DEHP is a commonly used plasticiser for PVC consumables. When incorporated in PVC, it can escape by evapouration or extraction by contact with liquids because it is not chemically bonded to the PVC.[19] This is due to the polar interactions between the ester groups and the aromatic ring of the phthalate molecule and the positively charged areas of the vinyl chain.[20] Pure DEHP has a vapour pressure of 1.43 x $10^{-7}$ mmHg at 25 °C.[21] It is expected that the vapour pressure of the DEHP emitted from DEHP incorporated PVC would be lower than that of pure DEHP.[22] The measurement of DEHP is also of concern because adverse effects on human health have been expressed even for low level exposure.[23, 24] The chemical structures and vapour pressures for the tested compounds are given in Table 1. The test compounds were selected to represent a range of different vapour pressures and functional groups in order to test the limit of detection (LOD) and the selectivity of the sensor.

**Table 1** Chemical structure and vapour pressure (at 25°C) of tested compounds.

| Compound (abbreviation) | Vapour pressure at 25 °C/ mm Hg | Chemical structure |
|---|---|---|
| Bis(2-ethylhexyl) phthalate (DEHP) | 1.43 x $10^{-7}$ [a] | 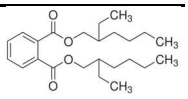 |
| 3-dinitrobenzene (1,3-DNB) | $2\times10^{-4}$ [b] | 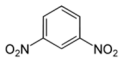 |
| 1-chloro-2,4-dinitrobenzene (CNDB) | 0.001 [b] | 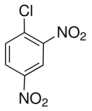 |
| 2,4-dinitrotoluene (2,4-DNT) | 0.002 [b] | 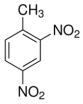 |
| 2-naphthalenethiol | 0.005 [b] | 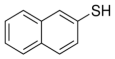 |
| 4-methyl-2-nitrophenol | 0.04 [b] | 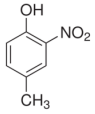 |
| 4-nitrotoluene | 0.1 [b] | 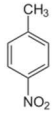 |

[a] Reference 19

[b] Royal Chemical Society chemical structure data base

## Experimental section

### Materials

1,3-dinitrotoluene, 1-chloro-2,4-dinitrobenzene (97% purity), 2,4-dinitrotoluene (97% purity), 2-naphthalenethiol (99% purity), 4-methyl-2-nitrophenol (99% purity), 4-nitrotluene were purchased from Sigma-Aldrich Australia. Tygon® formula R-3603 laboratory tubing (containing DEHP phthalate as per product description) was purchased from Sigma-Aldrich Australia.

### Sputtered-gold film preparation

Gold (99.99%) was sputtered onto clean silicon substrates using a Leica EM SCD005 sputter coater under argon. The vacuum chamber was evacuated to 0.05 mbar and the sputter coating attachment was charged at 30 mA with an argon carrier gas. The silicon substrates were placed 50 mm from the gold source. The sputtering time was 150 s. This results in a gold coating of approximately 30 nm with a root-mean-square surface roughness of 5.5 nm measured by atomic force microscopy (AFM). Gold sputter target was purchased from ProSciTech.

### Atomic Force Microscopy measurements

Sputtered gold films were imaged at room temperature in ambient atmosphere with an atomic force microscope (NT-MDT) in contact mode. The cantilever used was a silicon cantilever with platinum coating (NT-MDT, CSG11/Pt/20).

### Raman Spectroscopy

Raman measurements were carried out at room temperature using a Renishaw inVia Raman Microscope. All spectra were acquired with a 50× magnification objective, 10 s exposure of 20 mW of 785 nm excitation and acquisition time of 30 s.

### X-ray photospectroscopy analysis

XPS spectra were acquired using a Kratos Axis Ultra photoelectron spectrometer which uses Al Kα (1253.6 eV) x-rays with a pass energy of 20 eV and a spot size of 700 × 300 μm.

### Vapour detection test

Fig. 1a shows the schematics of the flow-through system. 1 mg of the compound to be tested is transferred into a 50 μl aluminium sample pan and placed inside the analyte chamber. The analyte chamber follows the basic cyclone design using the benefit of swirl flow.[25] The swirling flow field inside the chamber is created by the addition of baffles on the inside of the chamber walls creating a turbulent flow which makes the vapour concentration constant and uniform inside the system. The system was flushed with dry nitrogen prior to use. The carrier gas (nitrogen) stream enters from the bottom of the

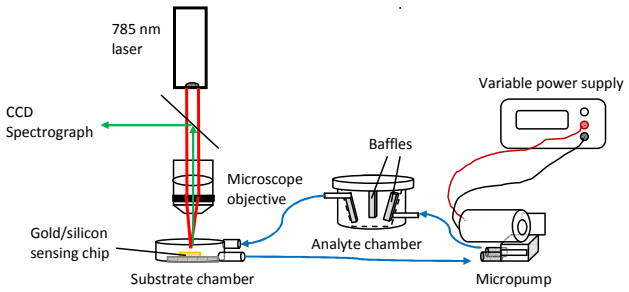


**Fig. 1** Schematic diagram of the flow setup. Flow-through system used in conjunction with inVia Renishaw Raman microscope for vapour detection on a gold coated silicon substrate. Vapours from analyte sublimation inside the sample chamber are delivered to the substrate surface by a micropump and then excited with a 785 nm laser. The sensing information is obtained from the measured spectrum of the inelastically scattered photons due to molecular vibrations. The detection axis is the same as the laser beam axis, y.

chamber, spiraling upwards and outflows from the top of the chamber. As the nitrogen carrier gas flow is adjacent to the solid analyte surface, sublimation occurs and mass is transferred to the carrier gas stream. Thus the cyclone design ensures that the saturation concentration is reached faster.

The substrate onto which the vapour molecules are captured for detection consists of a 30 nm thick freshly sputtered gold film on a silicon wafer (5 × 5 mm). A micropump (RS Components) with a flow rate of 200 ml/min is used for delivering analyte to the substrate surface. The substrate chamber consists of a cell incorporating a glass window and is placed directly under an objective lens of a Renishaw inVia Raman microscope through which the laser beam is focused on the substrate and scattered light is collected for detection. A photograph of the sample and analyte chambers are shown in Fig. 1b. Fig. 1c shows the flow-system during a test. System evaluation was carried out by measuring the response of the gold substrate inside the analyte chamber after exposure to the analyte vapour at room temperature.

## Results and discussion

Fig. 2 shows the AFM images of the gold coated silicon substrate. The morphology of the sputtered film on silicon appear very similar to that of selective chemical etching of Ag from Ag/Au alloy films on planar substrates reported by Dixon *et al*.[26] The film does not appear homogeneous with clusters of round features of approximately 50 nm in diameter. This is typical of sputtered gold films as gold atoms tend to cluster into islands minimizing overall surface energy.[27]

Fig. 3a shows the Raman spectra for the gold coated silicon substrate with 785 nm excitation after exposure to 2,4-DNT at room temperature inside the flow system. The flow rate of the nitrogen carrier gas inside the system was 200 mL/min and the intensity of the signal was found to be independent of the flow rate range tested (100-380 mL/min), but could be improved if the measurement was taken 1 min after turning the pump off. This result is in agreement with the static measurement performed separately shown in Fig. 3b. The

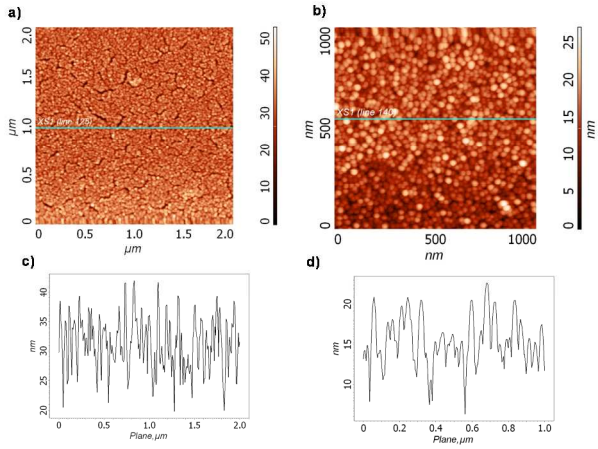


**Fig. 2** Contact mode AFM image of the sputter-deposited gold film on silicon used for the sensor in two different scan sizes: (a) and (b). (c) and (d) are line scans corresponding to the blue line in the AFM images above, showing the height of the structures from the sputtering process.

fact that the signal from the dynamic measurement is weaker and noisier is attributed to the interaction between the molecule and the gold surface. When the pump is switched on, the molecules are being swept over the surface of the substrate due to its motion in the flow, thus limiting the probability of the vapour molecules colliding with the substrate for adsorption and detection. In the static measurement, the mobility of the vapour molecules is reduced and there is sufficient time for adsorption to occur hence producing a detectable signal.

The responses of the other nitro analytes tested in the flow system are shown in Fig. 3b-e. Results were recorded with the pump turned off after recirculating the vapour for 5 mins at room temperature. The intense peak at 1380 $cm^{-1}$ seen in all four spectra is attributed to the symmetric stretching of the nitro group ($-NO_2$) and it reflects the interaction between the nitro group and the gold surface. It has been shown by electron energy loss spectroscopy and temperature programmed desorption that $NO_2$ adsorbs to the surface of gold through its oxygen atoms to form a bidentate surface chelate.[28] Upon adsorption, the valence electrons of the oxygen in the $NO_2$ group change the metal surface electron distribution close to the highest occupied molecular orbital in the valence band. The degeneracy at the surface is lifted by interaction of these lobes causing the band to be more intense than other bands in the spectrum. The broadness of the peak suggests intermolecular interactions between the DNT molecules on the gold surface.

For 2-naphthalenethiol (Fig. 3f), there is no difference between the static and the dynamic measurement in terms of signal strength. All bands in the dynamic and static spectra appear very narrow and sharp. The position of the bands for the adsorbed 2-napthalenethiol closely matches those for the pure solid. This means that the vibrational frequencies that are most visible in the spectra are not affected much by surface binding. Noticeable differences between the sensor response spectrum and the reference spectrum are the change in intensities for the ring deformation modes at 767, 514 and 354 $cm^{-1}$.[29] Probable adsorbed conformation of 2-naphthalenethiol on the gold surface is with the aromatic rings perpendicular to

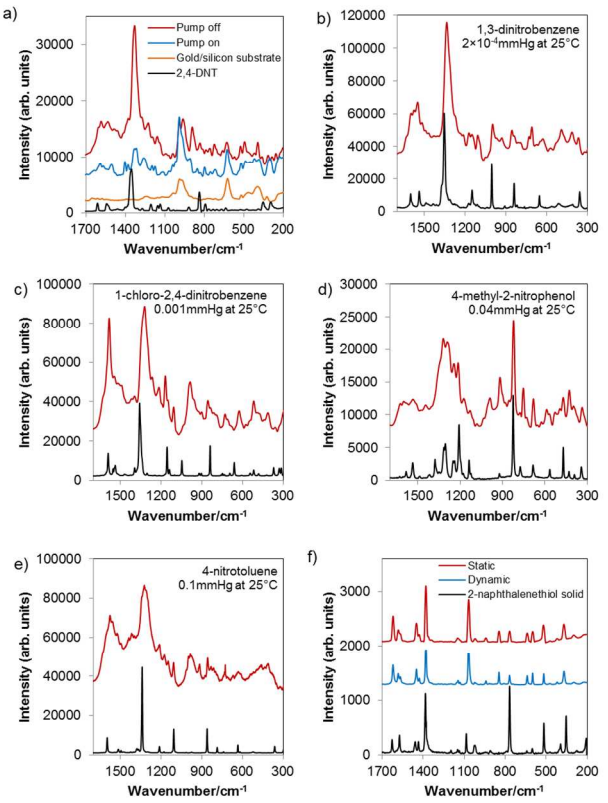


**Fig. 3** Raman spectra of six different compounds detected in the flow system on a sputtered gold coated silicon substrate at room temperature. Dynamic response (blue) was recorded with the pump turned on at a flow rate of 200ml/min. Static response was recorded with the pump turned off after recirculating the vapour for 5 mins at room temperature. Spectra of the solid analyte (black) are also show for comparison. a) 2,4-dinitrotoluene, b) 1,3-dinitrobenzene, c) 1-chloro-2,4-dinitrobenzene, d) 4-methyl-2-nitrophenol, e) 4-nitrotoluene, f) 2-naphthalenethiol.

the metal surface[29] as the attachment of 2-napthalenethiol occurs via the Au-S bond. This covalent bond formation causes localized charge fluctuations at the metal-molecular interface inducing a series of dipoles,[30] probably the reason why the bands are so intense in comparison to 2,4-dinitrotoluene. Similar observations have also been made by Hill and Wehling.[31] They compared different molecules adsorbed on silver and gold surface and reported that *p*-mercaptoaniline gave significantly larger intensities than other non-thiol molecules tested. The sharpness of the bands probably points at relatively low inhomogeneous broadening, since the thiol group binds strongly to gold with the sulfur-gold interaction being the predominant mode. The sharpness of the Raman bands of thiol molecules has also been explained by the effective resonant model proposed by Ueba[8] that the electronic resonant level of the adsorbed molecule shifts towards lower energies and the effective resonant condition is realised even when the molecule is excited by the off-resonant energy of the isolated molecule.

The detection of DEHP emitted from a sample of Tygon® tubing is shown in Fig. 4a. Characteristic bands for phathalate esters at 1040, 1581, 1600 $cm^{-1}$ are associated with the various vibrations of the ortho-phenyl group[32] and the band at 1726 $cm^{-1}$ is assigned to the carbonyl C=O stretching

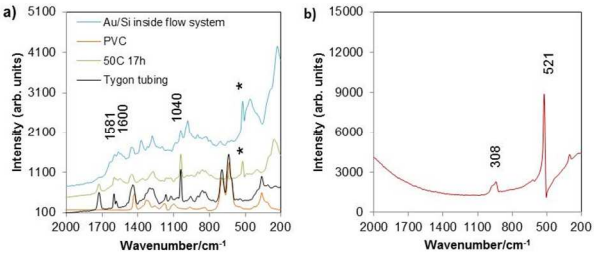


**Fig. 4** Raman spectra of a) the gold coated silicon substrate after exposure to a sample of Tygon® tubing inside the flow system at room temperature and a sealed cell at 50 °C. A spectrum of the Tygon® tubing and pure PVC powder are also shown for comparison. The * denotes peak due to the silicon underneath the gold. b) An uncoated silicon substrate after exposure to DEHP at 50 °C for 17 h.

vibration of the ester group. Measurement of DEHP from commercial PVC products by Uhde *et al*.[33] reported that, in general, DEHP emission from wallpaper measured in a CIS/GC-MS system results in a maximum concentration of approximately 1 $\mu g/m^3$ under ambient conditions. Thus this example shows that the LOD of our technique is at the level of sub-ppb, comparable to the detection level reported by Oo *et al*. and Piorek *et al*., demonstrated using pyridine and 4-nitrophenol. Further investigation to confirm DEHP on the gold surface was performed in a 0.75 ml stainless-steel sealed cell containing a sample of the PVC tubing and a gold coated silicon substrate. The cell was kept at 50 °C for 17 h to increase the DEHP concentration. As can be seen from Fig. 4a, the bands become more pronounced and the entire spectrum is a closer match to the spectrum of the PVC tubing than that obtained inside the flow system due to higher concentration of DEHP at higher temperature. The uncoated silicon (Fig. 4b) substrate shows no Raman bands that correspond to DEHP except for the main silicon band at 521 $cm^{-1}$, a weak peak at 308 $cm^{-1}$ corresponding to Si crystals,[34] and another weak broad band in the 900-1100 $cm^{-1}$ is the two phonon overtone of silicon.[35]

All compounds tested gave identifiable Raman signal with some showing more spectral difference in both relative intensity and band positions compared to the solid analyte. Most noticeably, 2-naphthalenethiol has a lower vapour pressure than 4-methyl-2-nitrophenol and 4-nitrotoluene, but out of all compounds tested, 2-naphthalenethiol gave the strongest signal on gold with its Raman spectrum closely resembling the spectrum recorded of the material alone. Furthermore, the static and the dynamic spectra for 2-napthalenethiol are almost the same; suggesting that a flow rate of 200 ml/min has no effect on the adsorption capacity of 2-naphthalenethiol. In contrast, the influence of the flow is more significant in the case of nitro analytes. Thus the LOD of the sensor could also be related to the molecule-gold interaction energies as well as the vapour pressure of the solid sample. Table 2 presents the bond enthalpy between the different functional groups and gold substrate for the three types of compounds studied in this work. From the table, 2-naphthalenethiol forms the strongest bond with gold compared to other compounds tested. In general, sulfur containing

compounds have strong specific interaction with gold and tend to chemisorb onto its surface resulting in a

**Table 2** Energetic of adsorption of different functional groups on gold surface

| Molecule | Nature of bonding | Interaction | Bond enthalpy Δ*H*, kJ/mol |
|---|---|---|---|
| 2-naphthalenethiol | Chemisorption | Sulfur-gold | 167[a] |
| Di(2-ethylhexyl) phthalate | Physisorption | π electrons –gold | 25[b] |
| | Van der Waals | ester-gold (through charge transfer coordination) | |
| 2,4-dinitrotoluene and other nitroaromatics tested | Dative bonding | Nitro-gold | 59[c] |

[a]reference 37, [b]reference 40, [c]reference 38

metal-S bond formation.[36] Estimated using alkanethiol adsorption, this bond energy is approximately 167 kJmol$^{-1}$.[37] For the nitro analytes, the bonding between the nitro group and the gold surface is dative through the interaction between the oxygens on the nitro groups and the gold surface. This interaction has been estimated to be 59 kJmol$^{-1}$.[38] As for DEPH, the adsorption is a physisorption through the aromatic π electrons and the gold surface,[39] this interaction energy is only about 25 kJmol$^{-1}$.[40] Van der Waals interaction between the ester group of the DEHP and the gold can also occur. Of all compounds tested, DEHP has the lowest vapour pressure at room temperature and the weakest interaction with gold. The detected DEHP Raman intensity was also the lowest amongst all compounds tested. This result suggests interaction between the molecule and the gold substrate could be a critical parameter in detectability as well as the vapour pressure of the compound. In any case, the reference spectra were used as a guide only and exact match of the band positions were not expected. This is because vibrations of a molecule depend on its physical state and Raman scattering is proportional to the polarizability of the molecule.[8] While the detected signals of molecules are due to the adsorbed state, the references are of the pure material in the solid state. When a molecule is adsorbed on a surface, a new species is formed (molecule-metal complex). Hence a change in the electronic and the vibrational states is expected due to the rearrangement of the electron configuration of the molecule.[41] The resulting physical interaction between the molecule and the gold substrate, the electromagnetic field of the incident light is also modified by the surface in magnitude, direction, and spatial dependence.[42]

### Substrate contamination and storage

It has been observed that within minutes of exposure to the laboratory atmosphere, a clean hydrophilic gold surface can be rendered hydrophobic by adsorption of nonpolar contaminants.[43-47] The storage condition of the substrates is thus crucial as the reliability of the sensor could be compromised by surface fouling. Preserving the activity of the substrate for practical use was considered by studying different storage environments. In a static test, a significant decrease in signal intensity was observed for the air-exposed substrate which showed a 93% reduction in signal intensity. Identifiable signal was detected with the substrates stored in nitrogen atmosphere at room temperature and -20 °C (Fig. 5).

The decrease in the Raman intensity for the air exposed substrate indicates that the detection mechanism is sensitive to the surface chemistry of gold. While bulk gold is generally considered inert, nano-sized gold can form surface intermediates of moderate stability[48] thus causing unnecessary background which may interfere with signal readouts. A sputtered gold film on silicon was investigated by X-ray photoelectron spectroscopy within 2 hours of film preparation. The sample had been stored inside a 15 ml glass vial immediately after retrieving the sample from the sputter coater. Detectable oxygen and carbon species suggest organic contamination from the air inside the vial is evident in Fig. 6.

The O 1s signal at 532 eV is assigned to oxygen adsorbed on gold surface.[49] The value at 533 eV can be attributed to $Au(OH)_3$ or $Au_2O_3$[50, 51] as gold can be readily oxidized under ambient conditions.[52] However, for the majority of all known oxides or hydroxides, the binding energy of the oxygen 1s electron varies between 525 and 531 eV,[53] thus the oxygen peak at 530 eV provides indication but not conclusive evidence of the presence of gold oxide. To be sure, there should also be a peak at 85.7 eV in the gold 4f for the gold oxide. This was not observed, probably there was not enough gold oxide in the samples to be detected. Further evidence suggesting contamination is the Raman spectrum of the gold substrate without exposure to analyte shown in Fig. 3a. Bands at 1037,

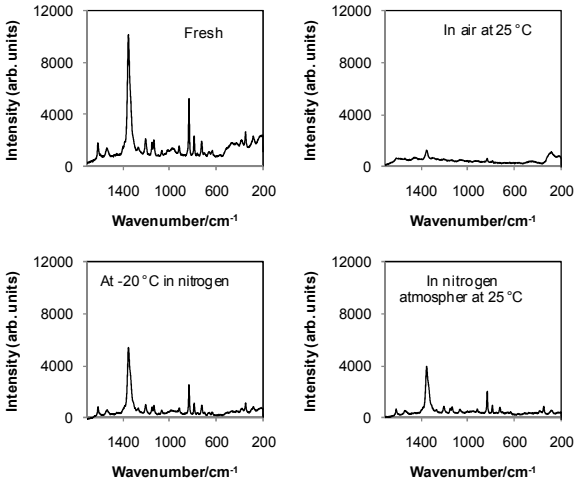


**Fig. 5** The effect of the storage condition on the Raman spectrum of 2,4-DNT on Au/Si substrates. In each case, the gold film was freshly prepared and stored under the specified condition for 24 h before exposing the substrate to 2,4-DNT vapours at room temperature.

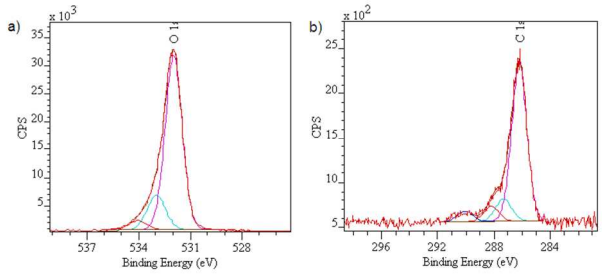


**Fig. 6** High-resolution XPS spectra of a) the O1s and b) the C1s photoelectrons of a gold coated silicon substrate. The spectra were acquired with a pass energy of 20 eV and a spot size of 700 × 300 µm.

982, 621, 388 and 289 $cm^{-1}$, are typical of carbonate[54, 55] and sulfate[56] species. Conveniently, these background signals do not interfere significantly with the detection of the selected analyte and can be distinguished from the signal response spectrum. Nevertheless, we recognize the importance of the cleanliness of the gold surface for obtaining unambiguous signals.

## Conclusions

This paper presents a vapour detection method using Raman spectroscopy. Differences in spectra were found between the static and the dynamic test measurements with the static measurement giving more pronounced bands.

We examined the effect on the Raman spectrum of three different bonding types with gold: van der Waals, dative and covalent bonding by comparing the quality of the spectrum obtained from three different types of compounds selected. As well as the vapour pressure of the compound, the detection of the vapour molecules on the surface of the gold coated silicon substrate appears to be dependent on the net physicochemical force which consists of: 1) the interaction strength between the molecule and the gold surface and 2) the dynamics in the flow system. The technique is suitable for detection of molecules that bear functional groups that will interact favourably with gold with a LOD of parts per million or greater for the nitro ananlytes tested and parts per billion for the DEHP emitted from PVC tubing. The current experiments were conducted within 1-5 mins because the gold film quickly ages when exposed to atmospheric conditions. This could be overcome by storing the substrates under inert atmosphere at low temperatures or vacuum until use as demonstrated in this work.

[a] *Central Analytical Research Facility (CARF), Institute for Future Environments Queensland University of Technology. Tel: 61 7 3138 9403; E-mail: alison.chou@qut.edu.au*
[b] *School of Chemistry, Physics and Mechanical Engineering Faculty of Science and Engineering, Queensland University of Technology. Tel: 61-7-31382275;*
[c] *Centre for Micro-Photonics, Faculty of Engineering and Industrial Sciences, Swinburne University of Technology, Australia. Fax: +61 3 9214 5435; Tel: +61 3 9214 8718; E-mail: sjuodkazis@swin.edu.au*

## Acknowledgement

The authors would like to thank Mr. Armin Leibhardt for fabricating the flow-through cells. Dr. Llew Rintoul for helpful discussions regarding Raman spectroscopy. Dr. Barry Wood for XPS analysis, QUT Central Analytical Research Facility. QUT electrical workshop. This work was supported by the Australian Research Council, Linkage Project LP0882614: a new nano-sensor technology for the detection and identification of residual vapours explosives, drugs and chemicals in the air.

## References

1. B. C. Dionne, D. P. Rounbehler, E. K. Achter, J. R. Hobbs and D. H. Fine, *Journal of Energetic Materials*, 1986, **4**, 447-472.
2. M. Fleischmann, P. J. Hendra and A. McQuillan, *Journal of Chemical Physics Letters*, 1974, **26**, 163.
3. D. L. Jeanmaire and R. P. Van Duyne, *Journal of Electroanalytical Chemistry and Interfacial Electrochemistry*, 1977, 1-20.
4. M. G. Albrecht and J. A. Creighton, *J Am Chem Soc*, 1977, **99**, 5215-5217.
5. D. A. Long, *The Raman Effect: A Unified Treatment of the Theory of Raman Scattering by Molecules*, John Wiley & Sons, Ltd, West Sussex, England, 2001.
6. M. Moskovits, *Notes Rec Roy Soc*, 2012, **66**, 195-203.
7. J. R. Lombardi, R. L. Birke, T. H. Lu and J. Xu, *J Chem Phys*, 1986, **84**, 4174-4180.
8. H. Ueba, *J Chem Phys*, 1980, **73**, 725-732.
9. T. Vo-Dinh and D. L. Stokes, *Field Anal Chem Tech*, 1999, **3**, 346-356.
10. D. A. Stuart, K. B. Biggs and R. P. Van Duyne, *Analyst*, 2006, **131**, 568-572.
11. J. Bowen, L. J. Noe, B. P. Sullivan, K. Morris, V. Martin and G. Donnelly, *Appl Spectrosc*, 2003, **57**, 906-914.
12. M. K. K. Oo, C. F. Chang, Y. Z. Sun and X. D. Fan, *Analyst*, 2011, **136**, 2811-2817.
13. J. M. Sylvia, J. A. Janni, J. D. Klein and K. M. Spencer, *Anal Chem*, 2000, **72**, 5834-5840.
14. J. Wang, L. L. Yang, S. Boriskina, B. Yan and B. M. Reinhard, *Anal Chem*, 2011, **83**, 2243-2249.
15. K. Kneipp, Y. Wang, R. R. Dasari, M. S. Feld, B. D. Gilbert, J. Janni and J. I. Steinfeld, *Spectrochim Acta A*, 1995, **51**, 2171-2175.
16. M. K. K. Oo, Y. B. Guo, K. Reddy, J. Liu and X. D. Fan, *Anal Chem*, 2012, **84**, 3376-3381.
17. B. D. Piorek, S. J. Lee, M. Moskovits and C. D. Meinhart, *Anal Chem*, 2012, **84**, 9700-9705.
18. A. Chou, E. Jaatinen, R. Buividas, G. Seniutinas, S. Juodkazis, E. L. Izake and P. M. Fredericks, *Nanoscale*, 2012, **4**, 7419-7424.
19. S. Vainiotalo and P. Pfaffli, *Ann Occup Hyg*, 1990, **34**, 585-590.
20. A. S. Wilson, *Plasticisers: principles and practice*, The Institute of Materials, London, 1995.
21. D. A. Hinckley, T. F. Bidleman, W. T. Foreman and J. R. Tuschall, *J Chem Eng Data*, 1990, **35**, 232-237.
22. A. Afshari, L. Gunnarsen, P. A. Clausen and V. Hansen, *Indoor Air*, 2004, **14**, 120-128.
23. S. Sathyanarayana, C. J. Karr, P. Lozano, E. Brown, A. M. Calafat, F. Liu and S. H. Swan, *Pediatrics*, 2008, **121**, E260-E268.

24. N. Hallmark, M. Walker, C. McKinnell, I. K. Mahood, H. Scott, R. Bayne, S. Coutts, R. A. Anderson, I. Greig, K. Morris and R. M. Sharpe, *Environ Health Persp*, 2007, **115**, 390-396.
25. A. K. Gupta, D. C. Lilley and N. Syred, *Swirl Flow*, Abaacs Press, Tunbridge Wells, England, 1984.
26. M. C. Dixon, T. A. Daniel, M. Hieda, D. M. Smilgies, M. H. W. Chan and D. L. Allara, *Langmuir*, 2007, **23**, 2414-2422.
27. C. Schug, S. Schempp, P. Lamparter and S. Steeb, *Surf Interface Anal*, 1999, **27**, 670-677.
28. M. E. Bartram and B. E. Koel, *Surf Sci*, 1989, **213**, 137-156.
29. R. A. Alvarez-Puebla, D. S. Dos Santos and R. F. Aroca, *Analyst*, 2004, **129**, 1251-1256.
30. G. Heimel, L. Romaner, J. L. Bredas and E. Zojer, *Phys Rev Lett*, 2006, **96**.
31. W. Hill and B. Wehling, *Journal of Physical Chemistry*, 1993, **97**, 9451-9455.
32. R. A. Nyquist, *Appl Spectrosc*, 1971, **26**, 81-85.
33. E. Uhde, M. Bednarek, F. Fuhrmann and T. Salthammer, *Indoor Air-International Journal of Indoor Air Quality and Climate*, 2001, **11**, 150-155.
34. Y. Kanzawa, S. Hayashi and K. Yamamoto, *J Phys-Condens Mat*, 1996, **8**, 4823-4835.
35. P. A. Temple and C. E. Hathway, *Physical Review B*, 1973, **7**.
36. R. G. Nuzzo, F. A. Fusco and D. L. Allara, *J Am Chem Soc*, 1987, **109**, 2358-2368.
37. R. G. Nuzzo, L. H. Dubois and D. L. Allara, *J Am Chem Soc*, 1990, **112**, 558-569.
38. J. Wang and B. E. Koel, *J Phys Chem A*, 1998, **102**, 8573-8579.
39. C. Woll, *J Synchrotron Radiat*, 2001, **8**, 129-135.
40. H. Dahms and M. Green, *Journal of The Electrochemical Society*, 1963, **110**, 1075-1080.
41. A. Campion and P. Kambhampati, *Chem Soc Rev*, 1998, **27**, 241-250.
42. S. Efrima, *J Chem Phys*, 1985, **83**, 1356-1362.
43. E. H. Loeser, W. D. Harkins and S. B. Twiss, *Journal of Physical Chemistry* 1953, **57**, 251-254.
44. G. L. Gaines, *J Colloid Interf Sci*, 1981, **79**, 295-295.
45. M. Schneegans and E. Menzel, *J Colloid Interf Sci*, 1982, **88**, 97-99.
46. T. Smith, *J Colloid Interf Sci*, 1980, **75**, 51-55.
47. C. D. Bain, E. B. Troughton, Y. T. Tao, J. Evall, G. M. Whitesides and R. G. Nuzzo, *J Am Chem Soc*, 1989, **111**, 321-335.
48. A. Haruta, *Chem Rec*, 2003, **3**, 75-87.
49. M. Peuckert, *Journal of Physical Chemistry*, 1985, **89**, 2481-2486.
50. M. Peuckert, F. P. Coenen and H. P. Bonzel, *Surf Sci*, 1984, **141**, 515-532.
51. T. Dickinson, A. F. Povey and P. M. A. Sherwoond, *Journal of the Chemical Society, Faraday Transactions 1: Physical Chemistry in Condensed Phases* 1975, **71**, 298-311.
52. M. White, *Journal of Physical Chemistry*, 1964, **68**, 3083-3085.
53. C. D. Wagner, D. A. Zatko and R. H. Raymond, *Anal Chem*, 1980, **52**, 1445-1451.
54. I. Pockrand and A. Otto, *Appl Surf Sci*, 1980, **6**, 362-371.
55. R. P. Cooney, M. R. Mahoney and M. W. Howard, *Chem Phys Lett*, 1980, **76**, 448-452.
56. K. H. Fung and I. N. Tang, *J Colloid Interf Sci*, 1989, **130**, 219-224.